The Journal of Physical Chemistry Letters
pubs.acs.org/JPCL Letter

Aluminum-Based Promotion of Nucleation of Carbon Dioxide Hydrates

Palash V. Acharya, Aritra Kar, Arjang Shahriari, Awan Bhati, Ashish Mhadeshwar, and Vaibhav Bahadur*

Cite This: *J. Phys. Chem. Lett.* 2020, 11, 1477−1482 Read Online

ACCESS | Metrics & More | Article Recommendations | SI Supporting Information

ABSTRACT: Gas hydrate formation has several applications in CO_2 sequestration, flow assurance, and desalination. Nucleation of hydrates is constrained by very high induction (wait) times, which necessitates the use of complex nucleation promotion techniques to form hydrates. Presently, we report the discovery of a simple, passive nucleation promotion technique, wherein *an aluminum surface significantly accelerates nucleation of CO_2hydrates*. Statistically meaningful measurements of induction times for CO_2 hydrate nucleation were undertaken using water droplets as individual microsystems for hydrate formation. The influence of various metal surfaces, droplet size, CO_2 dissolution time, and the presence of salts in water on nucleation kinetics was characterized. Interestingly, we observe nucleation initiation only on aluminum surfaces, the influence of which cannot be replicated by salts of aluminum. We discover that the aluminum−water interface is responsible for nucleation promotion. We hypothesize that hydrogen bubbles generated at the aluminum−water interface are responsible for nucleation promotion.

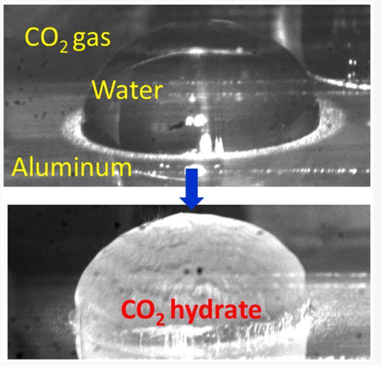

Clathrate hydrates are ice-like solids consisting of a lattice of hydrogen-bonded water molecules (host) encapsulating a guest molecule.[1,2] Gas hydrates (methane, carbon dioxide) form under high-pressure, low-temperature conditions. Formation involves nucleation of the first "cluster" of stable hydrate molecules followed by growth. Nucleation of hydrates is characterized by very long induction/wait times, typically ranging from hours to days, especially in a quiescent medium.[1] This challenge has been addressed via nucleation-promoting techniques such as the use of surfactants,[3,4] mechanical agitation,[5] quaternary ammonium salts,[6] and electronucleation[7−10] (by the corresponding author's group). Presently, *we show that aluminum strongly promotes nucleation of CO_2 hydrates*. Our finding about nucleation promotion at the aluminum−water (with dissolved CO_2) interface enables a novel technique for passive promotion of hydrate nucleation.

Presently, experiments on CO_2 hydrate nucleation were conducted using water droplets in CO_2 ambient in a high-pressure cell. While a majority of studies form hydrates from bulk liquid−gas mixtures, the use of droplets allows conducting multiple experiments in one run. Each droplet acts as an independent system, making it possible to obtain statistically significant data, bearing in mind that nucleation is stochastic and that hydrate formation experiments are usually very long. The use of droplets/bubbles to study nucleation and formation of hydrates[11−17] and ice[18,19] is widely employed. This approach also enables high-quality visualization of kinetics and crystal growth.

A schematic of our experimental setup is depicted in Figure 1 (pictures in the Supporting Information). A custom-built, nonstirred, 450 mL pressure vessel (Parr Instruments) with sapphire windows was used. Deionized (DI) water droplets (equal volumes unless specified otherwise) were dispensed on horizontally mounted metal plates in the vessel. New metal plates and droplets were used for every experiment to avoid the possibility of changes in surface chemistry/morphology and to avoid the memory effect. Up to three such plates (with 2−6 droplets on each) could be accommodated inside the pressure vessel in a single experiment. The pressure vessel was placed in an environmental chamber (ESPEC) to cool it to hydrate formation temperatures. Droplets were monitored with a high-speed camera (Photron Fastcam) fitted with a macro lens (Tokina).

Four surfaces were studied in this work: aluminum, anodized aluminum, copper, and stainless steel (SS). All the metallic surfaces (Al, Cu, and SS) had a polished mirror-like texture to minimize the influence of surface roughness on nucleation promotion. The rms values of the surface roughness for Al, Cu, and SS plates were 40, 49, and 61 nm, respectively (surface roughness profiles are provided in the Supporting Information). The surfaces were covered to prevent contact with air; the protective covering was removed just prior to the experiments to minimize contamination and oxide formation.

The surface cleaning and experimental procedure is detailed in the Supporting Information. In summary, it involved pipetting multiple droplets onto the surface, followed by pressurization of

Received: November 25, 2019
Accepted: January 31, 2020
Published: January 31, 2020

https://dx.doi.org/10.1021/acs.jpclett.9b03485
J. Phys. Chem. Lett. 2020, 11, 1477−1482

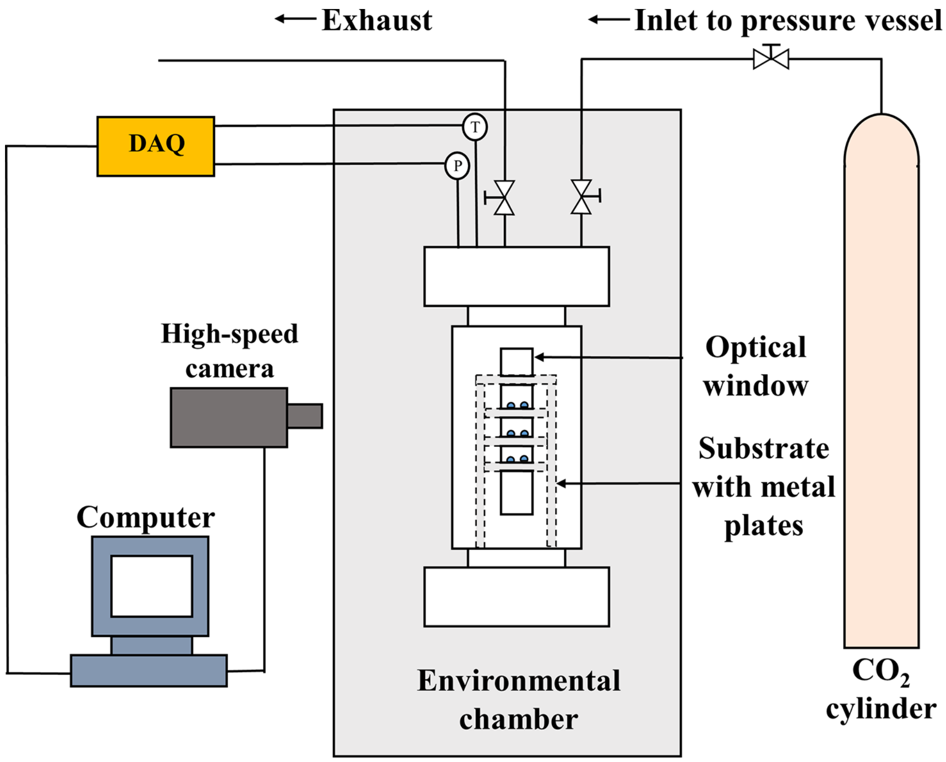

Figure 1. Schematic illustration of the experimental apparatus.

the chamber with 99.99% purity CO_2 (3 MPa) at 20 °C, and a dissolution time of 90 min (unless specified otherwise) to allow CO_2 diffusion into the water. Next, the chamber was cooled to 0.5 °C; a temperature higher than 0 °C was selected to eliminate the possibility of ice formation.

Nucleation was detected via continuous visualization; upon nucleation, the droplet turns opaque and the morphology changes as clearly seen in Figure 2 (video 1 in the Supporting Information). The induction time is calculated as the time when nucleation occurs after the droplets have entered the thermodynamically stable $p-T$ region for hydrate formation.[1] All experiments were stopped after 24 h.

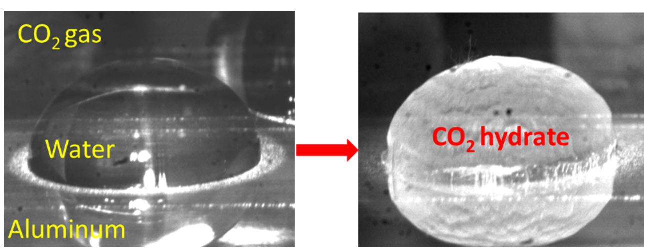

Figure 2. Water droplets (left) with a CO_2 dissolution time of 90 min turn opaque (right) upon conversion to CO_2 hydrates (right).

Table 1 summarizes the induction time measurements from this work; the reported induction time is the average of at least 25 droplets. In some previous studies,[11,12] the independence of nucleation events is questionable, since adjacent droplets were reported nucleating simultaneously. The observed sequence of droplet nucleation in our work was random in a spatial and temporal sense, which shows that the experimental approach did not compromise the stochastic nature of nucleation. The order of nucleation of droplets in the three-plate configuration is provided in the Supporting Information.

Key takeaways from Table 1 are highlighted ahead. *First, nucleation was observed only on the aluminum surface. No nucleation was ever observed on copper, stainless steel, or anodized aluminum surfaces within 24 h.* Induction times with Al showed a stochastic nature and ranged from 8 min to 22 h with every droplet eventually nucleating.

Second, the *mean induction time decreased, and the nucleation rate increased with increasing droplet volume.* This can be attributed to more nucleation sites becoming available, noting that the three-phase line length and Al−water interfacial area will increase with volume. The similarity between the mean and standard deviation for induction times indicate an underlying exponential distribution. On the basis of classical nucleation theory,[20] the probability (P) for nucleation at a particular subcooling ($\Delta T = T_{eq} - T$) and pressure is given by $P(t) = 1 - \exp(-J^*t)$. J is the nucleation rate, which can be obtained by fitting the equation with experimental data (detailed in the Supporting Information). The graph showing droplet volume-dependent cumulative probability distribution for nucleation is included in the Supporting Information.

The data on nucleation can be more meaningfully analyzed using a histogram (Figure 3), which shows the fraction of droplets nucleating in different time interval bins for three droplet volumes. It is seen that an increase in the metal−droplet interfacial area (due to increasing droplet volumes) leads to more favorable (faster) nucleation trends. This is reflected in a narrower distribution in the fraction of nucleating droplets, which tends to concentrate toward regions of lower induction time intervals. Additional histograms are included in the Supporting Information.

Third, experiments with water containing 0.6 M sodium chloride (3.5 wt % NaCl, to mimic seawater concentration), showed a 53% increase in the mean induction time and a 34% reduction in the nucleation rate (20 μL droplets), compared to

https://dx.doi.org/10.1021/acs.jpclett.9b03485
J. Phys. Chem. Lett. 2020, 11, 1477−1482

Table 1. Summary of Induction Time Data for Various Experiments

surface	salt added to DI water	CO_2 dissolution time (min)	droplet volume (μL)	nucleation rate (min^{-1})	induction time (min)		
					mean	std dev	range
aluminum 5052	none	90	10	0.0018	494.1	353.6	20−1321
aluminum 5052	none	90	20	0.0032	296.6	230.7	27−1000
aluminum 5052	none	90	40	0.0048	194.2	163.7	8−617
aluminum 5052	none	1440	20	0.0019	501.7	402.7	21−1422
aluminum 5052	3.5 wt % NaCl	90	20	0.0021	453.1	405.1	8−1567
stainless steel (T316SS)	none	90	20		no nucleation		
stainless steel (T316SS)	0.0625−5 wt % $AlCl_3$	90	20		no nucleation		
stainless steel (T316SS)	0.0625−5 wt % $Al_2(SO_4)_3$	90	20		no nucleation		
stainless steel (T316SS)	3.5 wt % NaCl	90	20		no nucleation		
copper	none	90	20		no nucleation		
anodized aluminum	none	90	20		no nucleation		

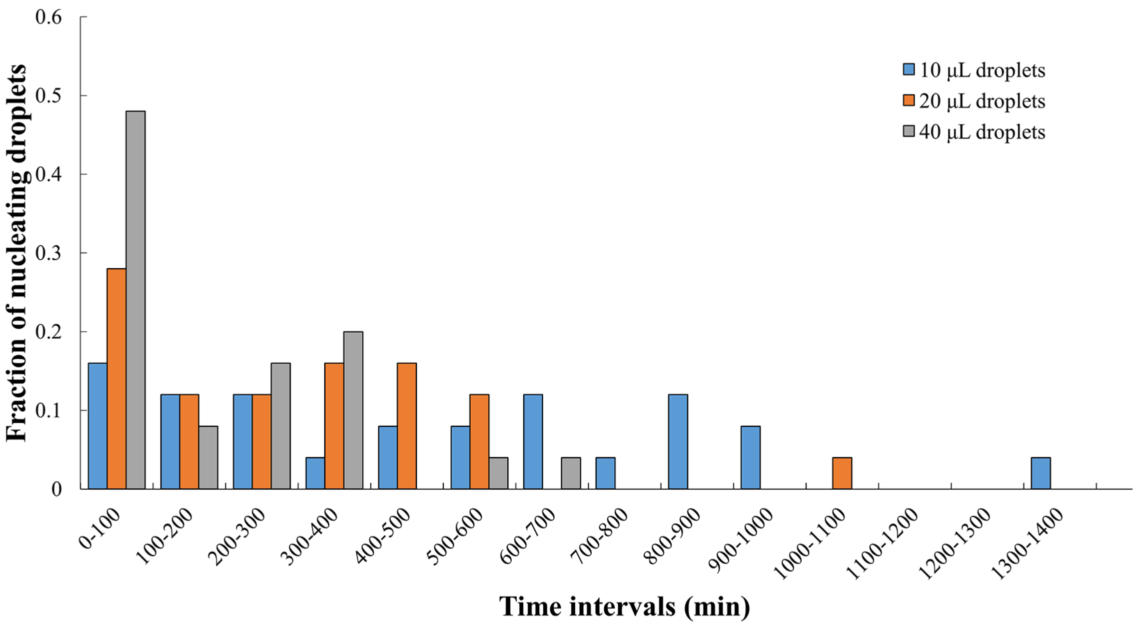

Figure 3. Histogram showing fraction of droplets nucleating in various time intervals (grouped using 100 min bins) for three different droplet volumes (10, 20, and 40 μL) (dissolution time: 90 min).

the results for DI water. This slower nucleation in the presence of salt is consistent with previous observations.[1] Salt ions in aqueous solutions attract water dipoles via Coulombic bonds (much stronger than hydrogen bonding or van der Waals forces), which reduces the availability of water molecules to form hydrates.[1] Importantly, Al surfaces still succeeded in promoting nucleation in saltwater solutions. *This repetition of a previously known phenomenon strengthens the scientific rigor of our approach.*

Another interesting finding of this study concerns the influence of the droplet CO_2 content on the nature of the hydrates formed. Experiments were conducted with water droplets staying in high-pressure CO_2 for 24 h (instead of 90 min) prior to cool-down. This extended time allows the droplet to completely saturate with CO_2 (diffusion constant of CO_2 in water[21] at 298 K is 1.92×10^{-9} m^2/s, which implies a mass diffusion length of 25.7 mm in 24 h vs 6.4 mm in 90 min). While the induction time increased for the higher dissolution time case, the most striking contrast from the 90 min dissolution time was the morphology of the resulting hydrates. Much more vigorous growth was observed for the 24 h dissolution time case, with hydrate "whiskers" seen protruding out of the droplets (Figure 4 and video 2 in the Supporting Information). This can be attributed to higher initial CO_2 concentrations, which enhances diffusion post nucleation, as the CO_2 dissolved in the interior diffuses toward the hydrate shell. Similar whisker-like growth has been observed previously on droplets subjected to a high driving pressure.[11]

Another *key finding from our experiments concerns the location of the hydrate nucleation sites.* Previous studies on hydrate formation report[22,23] that nucleation is triggered at the gas−liquid interface due to higher mole fractions of the guest molecule at the interface (at least 2 orders of magnitude higher than the bulk phase). In droplet-based nucleation experiments of hydrates[14,24] and ice,[18,19] nucleation is always observed at the gas−liquid interface or three-phase line, since the nucleation probability is higher than in the other regions of the droplet.

To determine the nucleation sites, experiments were conducted using cuvettes containing 1.75 mL of DI water,

https://dx.doi.org/10.1021/acs.jpclett.9b03485
J. Phys. Chem. Lett. 2020, 11, 1477−1482

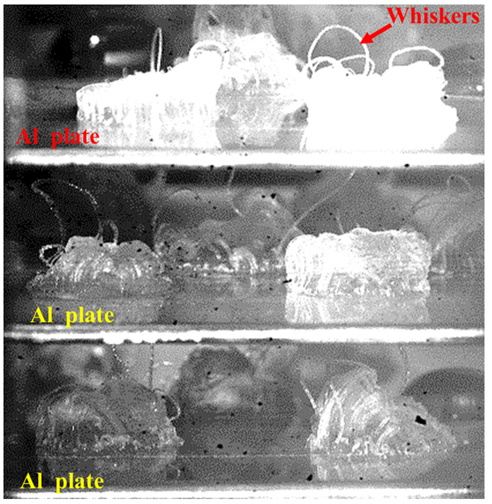

Figure 4. CO_2 hydrates (with whiskers) formed from water droplets with a long CO_2 dissolution time (24 h).

with an Al plate dipped as-per two configurations: (i) partially submerged longer plate with a three-phase contact line and (ii) a completely submerged shorter plate without a three-phase line. Baseline experiments were conducted without any plates and with a stainless steel plate; no nucleation was observed. In contrast, nucleation was observed on both configurations of Al plates. Most interestingly, nucleation was always initiated at the Al—water interface (in the interior of the liquid), even for the partially submerged plate configuration. This is shown in Figure 5 and is clearly evident in video 3 in the Supporting Information. This is a very interesting and nonintuitive finding, highlighting the role of the Al—water interface in nucleation promotion.

Our results clearly highlight the influence of aluminum in “catalyzing” nucleation in a CO_2-rich water solution, independent of the gas-phase CO_2. While specific mechanisms responsible for nucleation promotion will be investigated in future studies, this study reveals nucleation promotion as a consequence of bubbles generated due to reactions at the Al—water interface. Our line of reasoning for this hypothesis is briefly outlined ahead.

First, postexperiment surface examination shows visual discoloration of the surface. Evidence of a surface chemical reaction is further confirmed by a colorimetric indicator. Droplets were imbued with pyrocatechol violet (PV) indicator and placed on an Al substrate. PV is an indicator dye and chelates Al^{3+} ions to form a blue-violet colored coordination compound. Droplets turned blue shortly after contacting the Al surface, confirming the presence of Al^{3+} ions (video 4 in the Supporting Information). Previous studies[25,26] show that solvation of Al^{3+} ions forms Al-based coordination compounds, most notably a hydroxo—aquo—aluminum coordination compound $[Al-(H_2O)_6]^{3+}$, leading to the synthesis of octahedral polynuclear complexes. It has been theorized (but not experimentally proven) that the resemblance of such structures to the lattice structure of ice[25] and hydrates[10] promotes nucleation.

However, the above hypothesis cannot explain the present results. Experiments were conducted (Table 1) with two Al salts ($Al_2(SO_4)_3$ and $AlCl_3$) dissolved in water in varying weight concentrations (0.0625, 0125, 0.25, 0.5, and 5 wt %). Both salts produce Al^{3+} ions in water. These experiments were conducted on inert stainless steel to ensure the absence of surface-related nucleation. No nucleation was observed in any experiments, despite the presence of Al^{3+} ions.

The nucleation-promoting Al plates have a 2−10 nm[27] thick native oxide layer. Such oxide layers are porous and hydrophilic and can be broken down by the weakly acidic solution (carbonic acid), thereby resulting in Al—water contact. Further insights emerge from similar experiments conducted on Al surfaces with

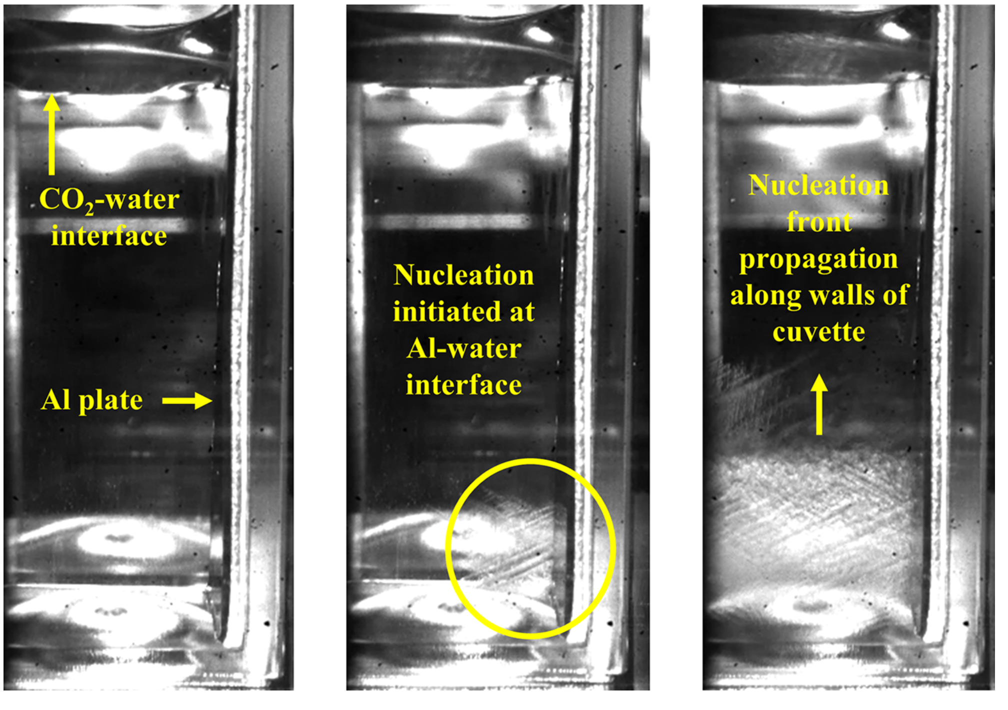

Figure 5. Snapshots depicting CO_2 hydrate nucleation at the Al—water interface (left to right). Nucleation originates at the spot, marked in yellow circle, and proceeds toward the three-phase line.

https://dx.doi.org/10.1021/acs.jpclett.9b03485
J. Phys. Chem. Lett. 2020, 11, 1477−1482

thicker oxide layers (anodized aluminum with 25 μm thick oxide layer, deposited via electrolytic oxidation). Interestingly, no nucleation was observed (Table 1) on such surfaces. Although anodized Al is porous on the outside, it is not porous throughout the oxide layer and prevents water contact with the Al surface. The absence of nucleation on anodized Al suggests that Al−water contact is necessary for nucleation.

We hypothesize that the likely cause of nucleation promotion is not directly related to the ionic species generated at the interface. Instead, hydrogen (H_2) bubble generation at the surface is likely responsible for nucleation. It has been reported that hydrogen nanobubbles form at the surface of a platinum electrode; the resulting high Laplace pressure generated due to the small radii leads to favorable conditions for the formation of hydrogen hydrates.[28] Our previous work showed bubbles assisting the nucleation of tetrahydrofuran hydrates.[9,10] Presently, Al reacting with carbonic acid/water will lead to generation of H_2 bubbles, which seed the nucleation of CO_2 hydrates. Carbonic acid will also assist in breaking down any thin or native oxide layers to promote Al−water contact. Our hypothesis is also backed by the lack of nucleation on Cu surfaces. Cu is less electropositive than Al and does not easily undergo displacement reactions to generate H_2 which would lead to bubble formation. It is noted that detecting such bubbles visually or via in situ spectroscopy is challenging since these experiments are carried out in a high-pressure cell, and the concentrations of any species will be low. Additional related evidence in support of the proposed mechanism lies in Figure 3, wherein the increased Al−water interfacial area (and therefore more nucleation sites containing H_2 bubbles) for higher droplet volumes leads to a narrower distribution in the fraction of nucleating droplets. This suggests a causal relation between interfacial area enhancement and nucleation promotion.

Interestingly, the proposed nucleation mechanism suggests that Al might not be as good of a nucleating agent for CH_4 hydrates as compared to CO_2 hydrates. The solubility of CH_4 in water is much lower than that of CO_2, and the dissolved CH_4 will not result in the generation of carbonic acid, which can break down the native oxide layer to promote Al−water contact.

Finally, we state that while H_2 bubbles appear to be the most probable cause of nucleation promotion, it is likely that there are additional factors such as the roughness/texture at the micro/nano scale that could also promote nucleation.

In conclusion, this study presents a simple, passive, and novel approach to promote nucleation of CO_2 hydrates. Importantly, this work lays the foundation for further studies on metal-mediated hydrate nucleation.

■ ASSOCIATED CONTENT

Supporting Information

The Supporting Information is available free of charge at https://pubs.acs.org/doi/10.1021/acs.jpclett.9b03485.

> (1) Images of experimental setup, (2) details of the experimental procedure, (3) surface roughness profiles for the metallic plates used in the present study, (4) confirmation of the stochastic nature of nucleation in our experiments, (5) comparison of droplet morphologies for different dissolution times of CO_2, (6) calculation of nucleation rate with graph of cumulative probability distribution, and (7) histograms showing fraction of droplets nucleating at different time intervals (PDF)
>
> Movie showing CO_2 hydrate formation on an Al surface (sped up by 7700×) (AVI)
>
> Movie showing hydrate nucleation and growth on an Al surface with CO_2 dissolution time of 24 h (sped up by 4900×) (AVI)
>
> Movie corresponding to Figure 5 showing nucleation occurring at the Al−water interface (sped up by 5800×) (AVI)
>
> Movie showing indicator experiments to detect Al^{3+} ions in water (sped up by 100×) (AVI)

■ AUTHOR INFORMATION

Corresponding Author

Vaibhav Bahadur − *Walker Department of Mechanical Engineering, The University of Texas at Austin, Austin 78712, Texas, United States*; orcid.org/0000-0001-7442-7769; Email: vb@austin.utexas.edu

Authors

Palash V. Acharya − *Walker Department of Mechanical Engineering, The University of Texas at Austin, Austin 78712, Texas, United States*

Aritra Kar − *Walker Department of Mechanical Engineering, The University of Texas at Austin, Austin 78712, Texas, United States*

Arjang Shahriari − *Walker Department of Mechanical Engineering, The University of Texas at Austin, Austin 78712, Texas, United States*

Awan Bhati − *Walker Department of Mechanical Engineering, The University of Texas at Austin, Austin 78712, Texas, United States*

Ashish Mhadeshwar − *ExxonMobil Research and Engineering, Annandale 08801, New Jersey, United States*

Complete contact information is available at: https://pubs.acs.org/10.1021/acs.jpclett.9b03485

Notes

The authors declare no competing financial interest.

■ ACKNOWLEDGMENTS

Work on CO_2 hydrates was supported by ExxonMobil through its membership in The University of Texas at Austin Energy Institute. This acknowledgment should not be considered an endorsement of the results by ExxonMobil. V.B. acknowledges NSF-CBET grant 1653412 for partial support of this work.

■ REFERENCES

(1) Sloan, E. D.; Koh, C. A. *Clathrate Hydrates of Natural Gases*, 3rd ed.; CRC Press/Taylor- Francis: Boca Raton, FL, 2007.

(2) Englezos, P. Clathrate Hydrates. *Ind. Eng. Chem. Res.* **1993**, *32* (7), 1251−1274.

(3) Kumar, A.; Bhattacharjee, G.; Kulkarni, B. D.; Kumar, R. Role of Surfactants in Promoting Gas Hydrate Formation. *Ind. Eng. Chem. Res.* **2015**, *54* (49), 12217−12232.

(4) Ganji, H.; Manteghian, M.; Sadaghiani zadeh, K.; Omidkhah, M. R.; Rahimi Mofrad, H. Effect of Different Surfactants on Methane Hydrate Formation Rate, Stability and Storage Capacity. *Fuel* **2007**, *86* (3), 434−441.

(5) Li, A.; Jiang, L.; Tang, S. An Experimental Study on Carbon Dioxide Hydrate Formation Using a Gas-Inducing Agitated Reactor. *Energy* **2017**, *134*, 629−637.

(6) Babu, P.; Linga, P.; Kumar, R.; Englezos, P. A Review of the Hydrate Based Gas Separation (HBGS) Process Forcarbon Dioxide Pre-Combustion Capture. *Energy* **2015**, *85*, 261−279.

(7) Park, T.; Kwon, T.-H. Effect of Electric Field on Gas Hydrate Nucleation Kinetics: Evidence for the Enhanced Kinetics of Hydrate Nucleation by Negatively Charged Clay Surfaces. *Environ. Sci. Technol.* **2018**, *52* (5), 3267−3274.
(8) Acharya, P. V.; Bahadur, V. Fundamental Interfacial Mechanisms Underlying Electrofreezing. *Adv. Colloid Interface Sci.* **2018**, *251*, 26−43.
(9) Carpenter, K.; Bahadur, V. Electronucleation for Rapid and Controlled Formation of Hydrates. *J. Phys. Chem. Lett.* **2016**, *7* (13), 2465−2469.
(10) Shahriari, A.; Acharya, P. V.; Carpenter, K.; Bahadur, V. Metal-Foam-Based Ultrafast Electronucleation of Hydrates at Low Voltages. *Langmuir* **2017**, *33* (23), 5652−5656.
(11) Servio, P.; Englezos, P. Morphology of Methane and Carbon Dioxide Hydrates Formed from Water Droplets. *AIChE J.* **2003**, *49* (1), 269−276.
(12) Lee, J. D.; Susilo, R.; Englezos, P. Methane-Ethane and Methane-Propane Hydrate Formation and Decomposition on Water Droplets. *Chem. Eng. Sci.* **2005**, *60* (15), 4203−4212.
(13) Ueno, H.; Akiba, H.; Akatsu, S.; Ohmura, R. Crystal Growth of Clathrate Hydrates Formed with Methane + Carbon Dioxide Mixed Gas at the Gas/Liquid Interface and in Liquid Water. *New J. Chem.* **2015**, *39* (11), 8254−8262.
(14) Saito, K.; Kishimoto, M.; Tanaka, R.; Ohmura, R. Crystal Growth of Clathrate Hydrate at the Interface between Hydrocarbon Gas Mixture and Liquid Water. *Cryst. Growth Des.* **2011**, *11* (1), 295−301.
(15) Servio, P.; Englezos, P. Morphology Study of Structure H Hydrate Formation from Water Droplets. *Cryst. Growth Des.* **2003**, *3* (1), 61−66.
(16) Jeong, K.; Metaxas, P. J.; Chan, J.; Kuteyi, T. O.; Aman, Z. M.; Stanwix, P. L.; Johns, M. L.; May, E. F. Hydrate Nucleation and Growth on Water Droplets Acoustically-Levitated in High-Pressure Natural Gas. *Phys. Chem. Chem. Phys.* **2019**, *21*, 21685−21688.
(17) Moudrakovski, I. L.; McLaurin, G. E.; Ratcliffe, C. I.; Ripmeester, J. A. Methane and Carbon Dioxide Hydrate Formation in Water Droplets: Spatially Resolved Measurements from Magnetic Resonance Microimaging. *J. Phys. Chem. B* **2004**, *108*, 17591.
(18) Carpenter, K.; Bahadur, V. Electrofreezing of Water Droplets under Electrowetting Fields. *Langmuir* **2015**, *31* (7), 2243−2248.
(19) Yang, F.; Shaw, R. A.; Gurganus, C. W.; Chong, S. K.; Yap, Y. K. Ice Nucleation at the Contact Line Triggered by Transient Electrowetting Fields. *Appl. Phys. Lett.* **2015**, *107* (26), 264101.
(20) Kashchiev, D.; Firoozabadi, A. Induction Time in Crystallization of Gas Hydrates. *J. Cryst. Growth* **2003**, *250* (3−4), 499−515.
(21) Cussler Edward Lansing Cussler, E. L. *Diffusion: Mass Transfer in Fluid Systems*, 2nd ed.; Cambridge university press, 2009.
(22) Rodger, P. M.; Forester, T. R.; Smith, W. Simulations of the Methane Hydrate/Methane Gas Interface near Hydrate Forming Conditions Conditions. *Fluid Phase Equilib.* **1996**, *116* (1−2), 326−332.
(23) Khurana, M.; Yin, Z.; Linga, P. A Review of Clathrate Hydrate Nucleation. *ACS Sustainable Chem. Eng.* **2017**, *5* (12), 11176−11203.
(24) Ueno, H.; Akiba, H.; Akatsu, S.; Ohmura, R. Crystal Growth of Clathrate Hydrates Formed with Methane + Carbon Dioxide Mixed Gas at the Gas/Liquid Interface and in Liquid Water. *New J. Chem.* **2015**, *39* (11), 8254−8262.
(25) Hozumi, T.; Saito, A.; Okawa, S.; Watanabe, K. Effects of Electrode Materials on Freezing of Supercooled Water in Electric Freeze Control. *Int. J. Refrig.* **2003**, *26* (5), 537−542.
(26) Hay, M. B.; Myneni, S. C. B. Geometric and Electronic Structure of the Aqueous $Al(H_2O)_6^{3+}$ Complex. *J. Phys. Chem. A* **2008**, *112* (42), 10595−10603.
(27) Hunter, M. S.; Fowle, P. Natural and Thermally Formed Oxide Films on Aluminum. *J. Electrochem. Soc.* **1956**, *103* (9), 482−485.
(28) Kashiwagi, K.; Hattori, T.; Samejima, Y.; Kobayashi, N.; Nakabayashi, S. Hydrogen Nanobubbles at Roughness-Regulated Surfaces: Why Does the Standard Hydrogen Electrode Need a Platinized Platinum Electrode? *J. Phys. Chem. C* **2019**, *123* (12), 7416−7424.

https://dx.doi.org/10.1021/acs.jpclett.9b03485
J. Phys. Chem. Lett. 2020, 11, 1477−1482